INTERNATIONAL JOURNAL OF PRECISION ENGINEERING AND MANUFACTURING Vol. 16, No. 12, pp. 2517-2527 NOVEMBER 2015 / 2517
DOI: 10.1007/s12541-015-0323-7 ISSN 2234-7593 (Print) / ISSN 2005-4602 (Online)

Process Optimization for Design of Duplex Universal Joint Fork using Unequal Thickness Flash

Chengliang Hu[1], Fan Zeng[1], Zhen Zhao[1,#], and Zengjun Guo[2]

1 Institute of Forming Technology & Equipment, Shanghai Jiaotong University, Shanghai 200030, China
2 Technical Center, Wangxiang Qianchao Co., Ltd., Hangzhou Zhejiang 311215, China
Corresponding Author / E-mail: zzhao@sjtu.edu.cn, TEL: +86-2162813430(ext.8116), FAX: +86-2162826575

KEYWORDS: Duplex fork, Crack, Flow velocity, Oxide scale, Finite element simulation, Optimization

To avoid defect formation, a two-step forging process for duplex fork was developed and optimized using an unequal thickness flash. The large cross-sectional difference between the different parts of the complex shape of the duplex fork made it difficult to forge. Crack defects formed during initial forging were observed and analyzed by finite element simulation, and the metal flow lines and velocity distributions on the main cross section were studied. A non-uniform velocity distribution with a large difference in the dangerous area and large amount of oxide scale most likely caused the crack defects. An optimized two-step forging process was developed, pre-upsetting was used to remove the oxide scale, and final forging using a die with an unequal flash gutter depth was used to obtain a reasonable velocity distribution. The effect of different process parameters on the optimized forging process was determined. The parameters included the pre-upsetting stroke, the friction factor, the workpiece mass, and the offset of the preform, and the results were used to improve the process stability. A duplex fork of acceptable quality and without any cracks was forged in successful trial production using the optimized process in the forging plant.

Manuscript received: June 9, 2015 / Revised: September 22, 2015 / Accepted: September 22, 2015

1. Introduction

Increasing global competitive pressure in the automobile industry has led to an increase in the demand for sound mechanical performance, fabrication efficiency, and process stability in the manufacture of automobile components. To improve their competitive ability and to meet market requirements, companies are attempting to shorten product redesign and development cycle times. Component die designs and process optimization strategies need to be accurate, effective, intuitive, and efficient.

The universal joint (also termed a Cardan, Hooke's, or U-joint) is used extensively in industrial applications and vehicle drivelines to connect misaligned shafts. It forms a mechanical connection between two shafts with interconnecting axes and provides a positive drive while allowing angular movement of one or both shafts. The duplex fork is a typical component of automobile universal joints. It consists of a four-legged spider or cross-fitted Y-shaped yoke on each shaft, as shown in Fig. 1. It functions under complex load conditions and needs to possess good mechanical properties.[1] Forging is therefore generally used to produce this component, rather than casting or machining.

Because of its complex shape, this component exhibits a high degree of deformation and complex material flow during forging. Consequently, defects such as underfilling and cracking are likely to occur during production.[2] Conventional defect analysis is usually based on experiments only, and conclusions are often drawn based on experience. However, some defects are difficult to explain, because the metal flow cannot be observed at all times.[3]

Finite element method (FEM) simulation enables observation of the formation and evolution of defects and is used extensively in forging-defect analysis. Damage analysis based on FEM simulation is an important method used to predict defect formation.[4,5] However, the simulation accuracy depends on the choice of appropriate damage model. Venugopal and Ramakrishnan[6] compared ten criteria used commonly in the engineering analysis of bulk formation, evaluated their accuracy and sensitivities, and found that none of the criteria is sufficiently accurate and universally applicable. The selection of appropriate damage models and their verification, or the development of new models is time consuming. Moreover, damage analysis is often applied to processes that include a cutting step or a fracture process. Furthermore, in hot-forging, the metal is normally hot and the tool is cool. The temperature varies dynamically with time and location in the metal. However, most existing damage models have been established

Fig. 1 Typical universal joint

for fixed temperatures, and cannot be used directly to predict and evaluate defects in hot forging.

Some researchers have analyzed the relationship between material flow velocity and metal defects. Using FEM and physical simulations, Arentoft et al.[7]analyzed flow line defects when forging with an H-shaped cross section. Joun et al.[8] simulated flow line formation in multi-pass axisymmetric forging using a rigid-viscoplastic FEM. Abdullah et al.[9] tried to explain defect risks in forging an autonomous underwater vehicle blade pin head based on observed cyclone-type material flow patterns. However, these studies focused on internal material flow, and external factors that may influence metal flow were ignored, for example oxide scale on the metal surface.

In hot forging, oxide scale is generated on metal surfaces in the presence of air. Because the oxide scale is located at the interface between the tool and the metal workpiece during hot-working, it influences the hot-working characteristics significantly.[10] Oxide scale improves lubrication between the tool and workpiece, and reduces friction during hot forging.[11] The oxide scale also affects metal heat conduction properties.[12] In recent years, the influence of oxide scale on metal flow has raised concerns. Suárez et al.[13] investigated the oxide layer deformation behavior of ultra-low carbon steel in plane strain compression. Because oxide scale thicknesses are small, their influence on material deformation is insignificant in large component hot forming in which the internal defects are mainly researched.[14] However, because automobile components are decreasing in size and increasing in accuracy, the influence of oxide scale on the hot-forging characteristics is becoming increasingly important in the manufacture of automobile parts using hot-forging methods.[15,16]

Flash thickness design is an effective method to improve material flow. Extensive research has been performed on the use of a fixed flash thickness in closed-die forging. The load and degree of die filling are significant factors that have been examined in these studies. Chavoshi et al.[17] investigated the effects of variable flash thickness on the strength of an AA7075 part obtained by hot closed-die forging and found that using a variable flash thickness die can increase the tensile strength of the forged parts significantly. However, the effects of unequal-thickness flash design on metal flow and defect formation needs to be understood further.

In this work, metal flow during forging of a universal joint duplex fork and the effect of oxide scale were investigated experimentally and by FE simulation. The main reasons for crack defect formation on the forging part are discussed in detail. An optimized two-step forging process with unequal-thickness flash design is proposed and the process stability is analyzed.

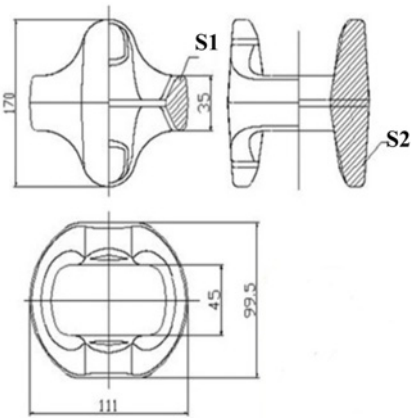

Fig. 2 Three-view diagram of duplex fork

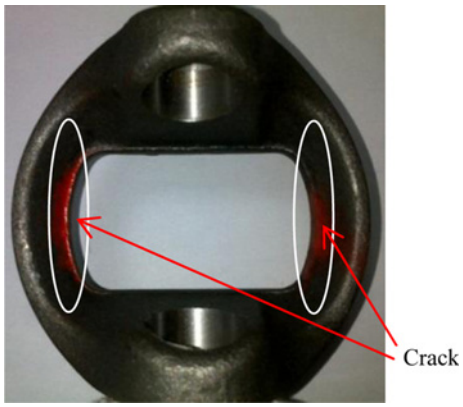

Fig. 3 Photograph of duplex forging part

2. Initial Forging Process

Three planes of a duplex fork are shown in Fig. 2. The part height ranges from 35 to 170 mm, with a 4.85-fold difference, and the cross section ranges from 753 (S1) to 4372 mm^2 (S2), with a 5.8-fold difference. A rod workpiece of 70.0 mm diameter and 100.0 mm length was used. The component raw material was 40Cr alloy (also termed 41Cr4 or AISI 5140), which is used extensively to manufacture various types of transmission parts such as gears, crankshafts, and steering knuckles.

2.1 Initial process

In the initial process, the component was produced using a 25 000 kN hot-die forging press by sawing, heating, forging, punching and trimming, peening, and heat treatment. One-step forging was used in the initial forging design to achieve a higher production efficiency. However, during production, cracks appeared after heat treatment in the area marked in Fig. 3. Ultrasonic flaw detection showed that the defect rate was over 20% and sometimes even 60% after forging. These small defects were enlarged by punching and could become sources of cracks

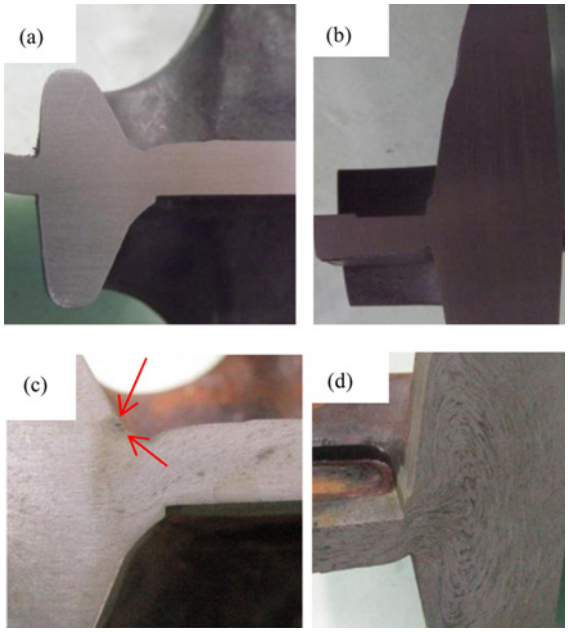

Fig. 4 Cross sections of forging parts: (a) cross-section s1 before corroding, (b) cross-section s2 before corroding, (c) cross-section s1 after corroding, and (d) cross-section s2 after corroding

during successive heat-treatment, which could lead to the formation of large cracks and useless products.

2.2 Crack observation

The initial forging process was studied experimentally to identify the cause of crack defects. In terms of the geometric shape of the component, the material distribution is uneven, which is unfavorable for material forming. Cross sections of the forging parts were studied to better understand the metal flow. As shown in Fig. 4(a) and (b), the forging parts were split into quarters along the symmetry planes and the cutting surfaces were polished. The polished surfaces were warm corroded with hydrochloric acid, and metal flow lines appeared on the cross sections, as shown in Fig. 4(c) and (d). No crack traces existed on the cross section of the fork part (S2), whether or not the part was corroded, whereas on the cross section of the rib part (S1), two slight crack traces appeared after corrosion of the forging parts, as indicated in Fig. 4(c).

2.3 FE analysis

2.3.1 Material modeling

A series of uniaxial hot-compression tests were performed using a computer-controlled Gleeble 1500 thermal mechanics simulator, to provide data for material modeling to support FE simulation of the forging process. Cylindrical specimens of 8.0 mm diameter and 12.0 mm length were prepared. Isothermal hot-compression tests were conducted at strain rates of 0.01, 0.1, 1, and 5 s^{1} from 950 to 1150°C in intervals of 50°C. The true stress–strain relationships of the 40Cr alloy at different temperatures and strain rates were investigated, as shown in Fig. 5.

The Arrhenius equation is often used to describe the relationship between flow stress, temperature, and strain rate, especially at high

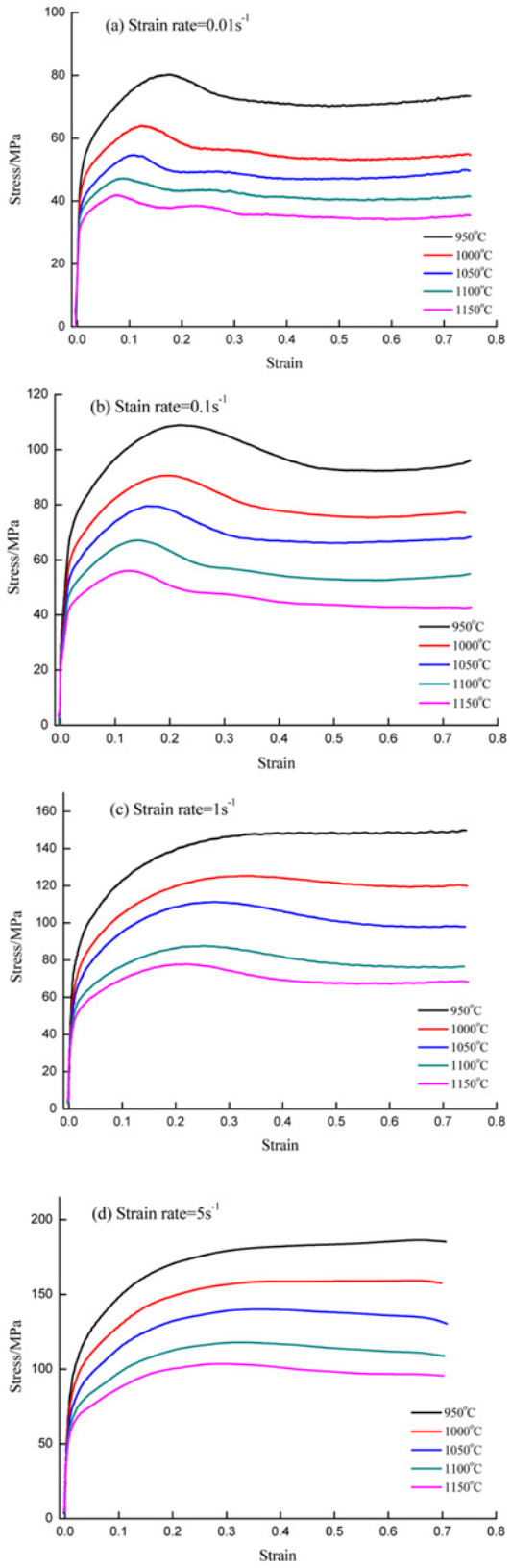

Fig. 5 Stress-strain relationships at different temperatures and strain rates

temperature. The effect of temperature and strain rate on deformation behavior can be represented by the Zener-Hollomon parameter Z in an exponential equation. The exponential and Arrhenius equations are

Table 1 Parameters of FE model

Parameters	Value	Unit
Forging speed	50	mm/s
Initial forging temperature	1100	°C
Preheating temperature of forging die	200	°C
Heat transfer coefficient (workpiece/tool)	1.5×10^4	W/(m^2·K)
Heat transfer coefficient (workpiece/environment)	150	W/(m^2·K)
Thermal capacity	824.9	J/(kg·K)
Friction factor	0.3	
Coefficient of expansion	13.32×10^6	

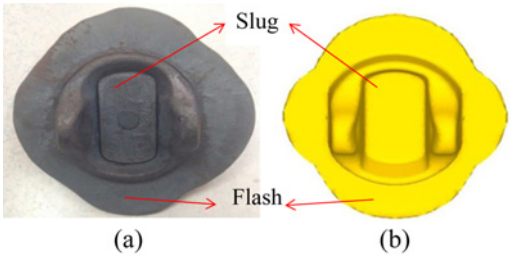

Fig. 6 Comparison of the shape of forged part: (a) shape in experiment, (b) shape in simulation

expressed as:

$$\dot{\varepsilon} = A[\sinh(\alpha\sigma)]^n \exp(-Q/RT) \quad (1)$$

where $\dot{\varepsilon}$ is the strain rate (s^1); Q is the apparent activation energy of deformation (kJ mol^1); R is the universal gas constant (8.31 J mol^1 K^1); s is the flow stress (MPa) for a given strain; and A, α, and n are the material constants.

From results of the isothermal hot-compression tests, the constitutive equation can be expressed as:

$$\dot{\varepsilon} = e^{25.8}[\sinh(0.010397\sigma)]^{5.28} \exp(-306373/8.31415T) \quad (2)$$

2.3.2 FE model

Hot forging of a duplex fork was simulated using the commercial FE code, DEFORM-3D. A 5.0-mm-thick slug in the middle (Fig. 6(b)) was punched after forging. Based on the symmetrical properties of the forging part, a quarter geometric model was used in the simulation to save computational time.

The simulation parameters are shown in Table 1. The upper forging die was set at 50 m/s, based on equipment conditions. The forging temperature and thermal conductivity were set based on practical process parameters. The friction factor between the workpiece and dies was set at 0.3.[18] The heat-transfer coefficients of the workpiece/tool and the workpiece/environment were set at 1.5×10^4 and 150 W/(m^2·K) respectively, based on previous research.[18] The thermal capacity was set at 824.9 J/(kg·K), and the coefficient of expansion was set at 13.32×10^6.[19]

2.3.3 Results and discussion

The experimental and simulated forging part shapes are shown in Fig. 6. Although the flash of the experimental forging is not completely symmetrical, there is good agreement between the experimental and simulated results. Therefore, the forging process was simulated successfully.

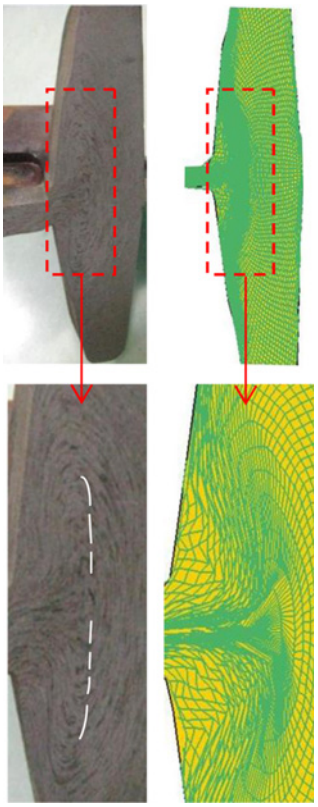

Fig. 7 Experimental and simulated flow line distributions

The lines on the cross section appear by corrosion after the forging was cut along the fork, and the flow line distribution on the cross section is also extracted from the simulated results, as shown in Fig. 7. The flow line distributions in the simulation are consistent with the experimental results. Three zones exist where many flow lines accumulate. This accumulation causes directionality of the flow line distribution. The tensile strength is high in the flow direction, and smaller perpendicular to the flow direction. In the accumulation zones, some flow lines bend inwards, which increases the risk of inner folding of the material.

The effective strain and temperature distributions for the simulation results are shown in Fig. 8. The strain on the flash at the rib side is relatively high. In particular, in the connecting region of the flash and rib (Fig. 8(a)), the strain is higher than that in the nearby area and greater than five. It can be inferred that the metal deformed strongly in this area. In contrast, the temperature in the slug area is lower than that in other regions and reaches 720°C, as shown in Fig. 8(b). This is because metal in this area contacts the die surfaces earlier than metal in other areas.

To understand the causes of defects, the metal flow velocity distribution on a specific cross section was drawn and analyzed. As shown in Fig. 9, cross-section S1 was selected for observation of the metal flow. In the final stages of forging, it is difficult for slug metal to flow to the outside, and the flow velocity in the transition region between the slug and rib is non-uniform. A large metal flow velocity

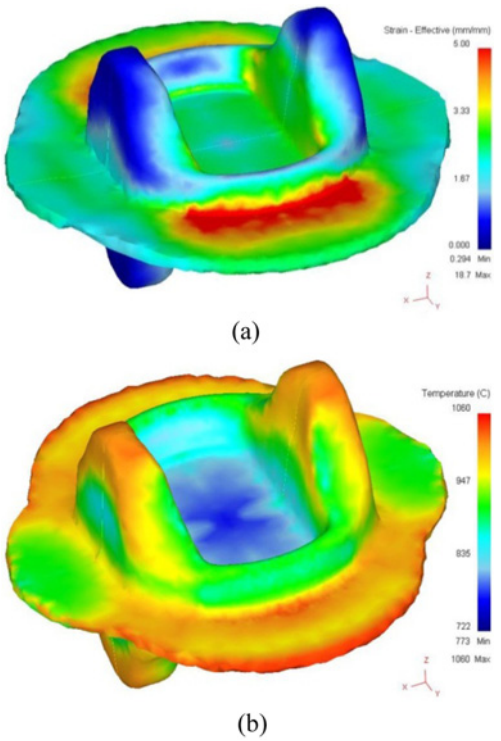

Fig. 8 Simulation results for initial process: (a) effective-strain distribution, (b) temperature distribution

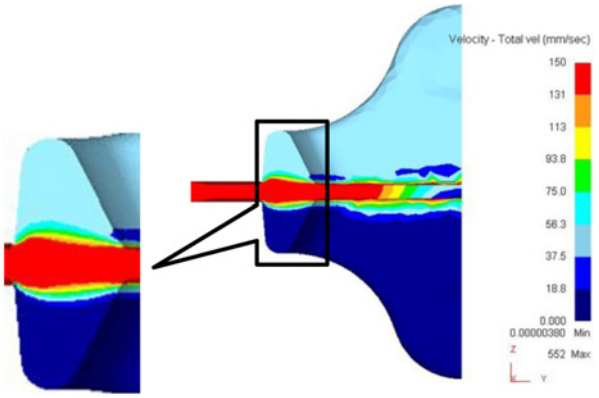

Fig. 9 Flow velocity at cross section

differential is created, and this increases the tensile stress inside the material, which leads to the appearance of cracks.

The large amount of material flowing in the region connecting the slug and the rib causes oxide scale flow, as shown in Fig. 10(a). During forging, the oxide scale is brittle and has no extension, therefore it cracks and separates easily, as shown in Fig. 10(b). Some hard oxide scale pierces the soft metal surface that bears a high-level tensile stress, and surface cracks form. In this case, cracks cannot be detected by the naked eye. However, after warm corroding, the oxide scale that was pierced in the forging part was corroded, and crack traces appeared. For this reason, crack traces can be detected after corrosion (Fig. 4(c)), but cannot be detected before corrosion (Fig. 4(a)). During forging, a large amount of oxide scale can influence the lubricating effect and die

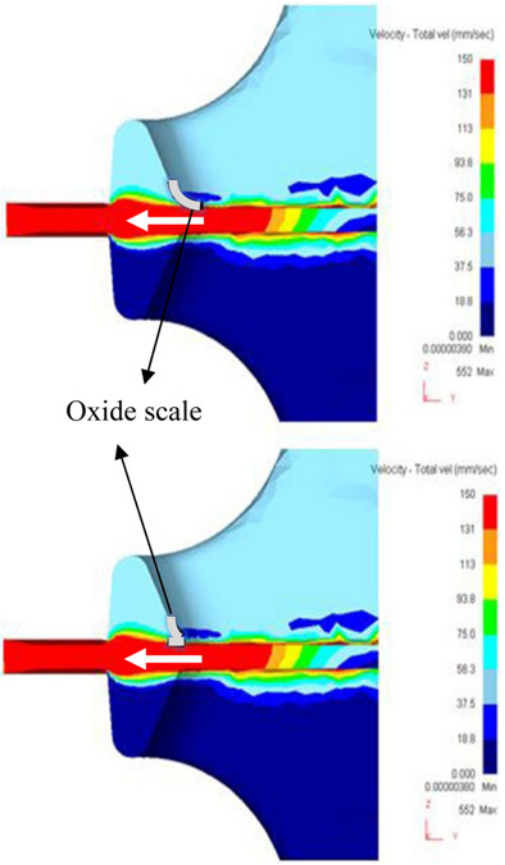

Fig. 10 Schematic diagram of oxide scale flow

filling conditions, and also increase the risk of surface crack formation of the forging part, especially under large metal flow velocity.

During the initial formation of the duplex fork, a non-uniform velocity distribution in the transition between the slug and the rib, and the large velocity difference led to the generation of additional tensile stresses, which then resulted in crack formation. A large amount of oxide scale was generated during one-step forging and the relatively harder oxide scale can increase the possibility of crack formation. After direct forging, punching and trimming were carried out, and the micro surface cracks formed during forging were enlarged.

3. Process Improvement Design

As discussed above, the large velocity difference between the non-uniform velocity distribution and the large amount of oxide scale are the main reasons for the formation of crack defects during initial forging of the duplex fork.

To reduce oxide scale, a two-step forging process including pre-upsetting and final forging was used instead of the initial one-step forging process. During pre-upsetting, most oxide scale that is generated in the heating process can be removed, which prevents the adverse effects of oxide scale on final forging. The pre-upsetting die is simple, easy to manufacture, convenient to use in production, and does not increase die costs significantly.

Although the risk from oxide scale was decreased by pre-upsetting,

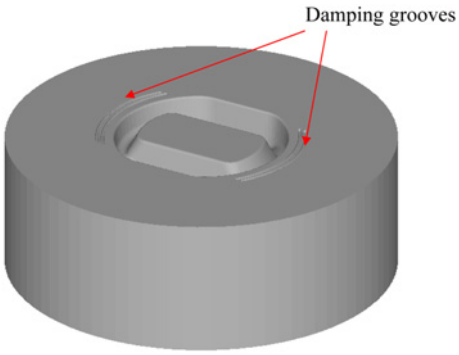

Fig. 11 Forging die with damping grooves

the problem of poor metal flow persisted, and the risk of crack formation was still high. During forging, large amounts of metal were required to fill the fork part of the die, whereas it was easy to form the rib part. The main flow of metal at the fork zone was in the axial direction to fill the corner of the fork, whereas the main flow in the rib zone was in the radial direction after the rib part had been formed over a short period. The metal flow velocity along the lower part was significantly larger than that on the other side. This resulted in a flow velocity difference, which led to a risk of defects. To change the flow mode, two solutions were proposed.

The first solution is to add damping grooves to increase the material flow resistance at the rib side of the dies, as shown in Fig. 11. Material flow to the outside in the radial direction becomes more difficult, and the corresponding velocity is reduced. The flow velocity difference in the cross-sectional area of the rib and the flash decreases significantly, whereas that in the cross-sectional area of the rib and slug decreased slightly, but was still high, as shown in Fig. 12(a).

The other solution is to design an unequal-thickness flash, using a slope transition between the fork and rib sides, so that the flash thickness at the fork zone is larger than that of the rib zone. The purpose of this design was to increase and decrease simultaneously the flow resistance along the rib side by thinner flash and along the fork side by thicker flash, respectively, to achieve a relative reasonable flow mode.

The Wolf equation can be used to design the flash region in hot-die forging. A fixed flash thickness die was designed using the Wolf relationship:[20]

$$h_f = 1.13 + 0.89\sqrt{m_F} - 0.017 m_F \quad (3)$$

where h_f is the flash thickness, and m_F is the mass of the part to be forged. The mass of the duplex fork is 3.02 kg. The calculated values for the flash thickness and width are 2.6 and 7.9 mm, respectively. Here, the flash thickness at the rib side is 2.6 mm, and that at the fork side is 5.2 mm. The detailed shape of the variation flash is shown in Fig. 13.

By using an unequal-thickness flash, the flow velocity difference in the cross-sectional area of the rib part and the flash remained large, whereas that in the cross-sectional area of the rib part and the slug decreased, as shown in Fig. 12(b).

To investigate the flow velocity distributions in the forgings, nine

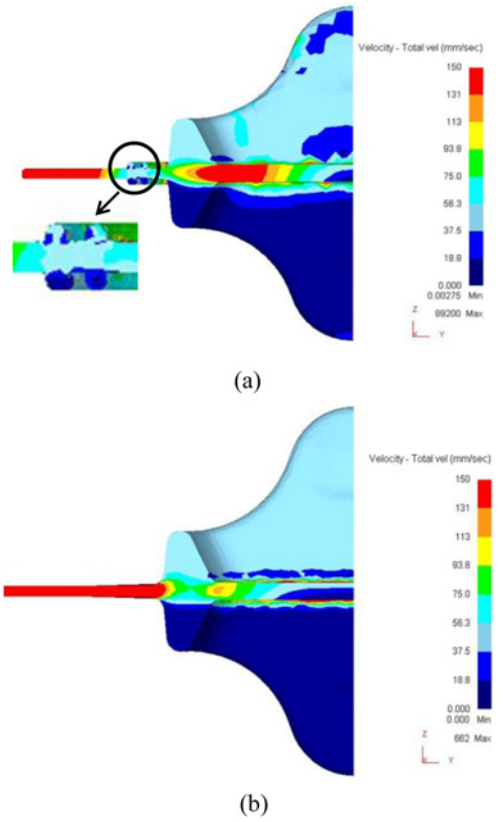

Fig. 12 Flow velocities for different designs: (a) design with damping grooves, (b) design with unequal thickness flash

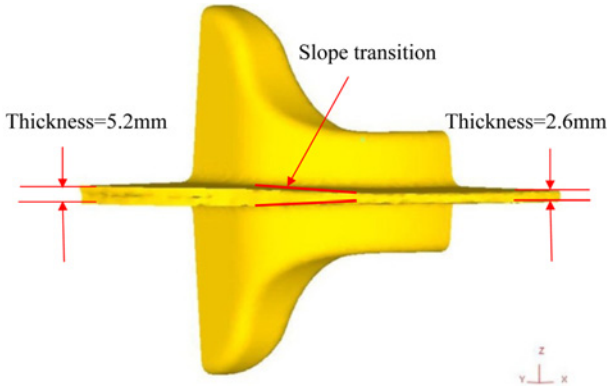

Fig. 13 Unequal thickness flash

representative points in the dangerous region were chosen and their flow velocities were collected and analyzed. As shown in Fig. 14, points 1 to 7 lie on one vertical line with 1 mm intervals and points 4, 8, and 9 lie on a central horizontal line with 2 mm intervals. The average velocity reflects the amount of metal flow in the radial direction, whereas the velocity gradient along the vertical line represents the extent of non-uniform velocity distribution in this region.

The velocities of selected points in the different designs are shown in Table 2. The average velocity in the design with damping grooves decreased from 176.8 to 163.2 mm/s, whereas that in the design with unequal thickness flash (UTF) decreased significantly, and had an

Table 2 Flow velocities of selected points in different designs

Design schemes	Velocity at different points (mm/s)									
	P1	P2	P3	P4	P5	P6	P7	P8	P9	Average
Design with damping grooves	91.6	153.4	187.0	196.9	189.2	165.1	104.1	221.3	159.8	163.2
Design with unequal flash thickness	50.2	74.3	99.6	99.8	96.7	77.3	55.2	117.6	78.8	83.3
Initial design	105.4	173.1	206.1	214.8	202.4	163.1	82.2	268.9	175.1	176.8

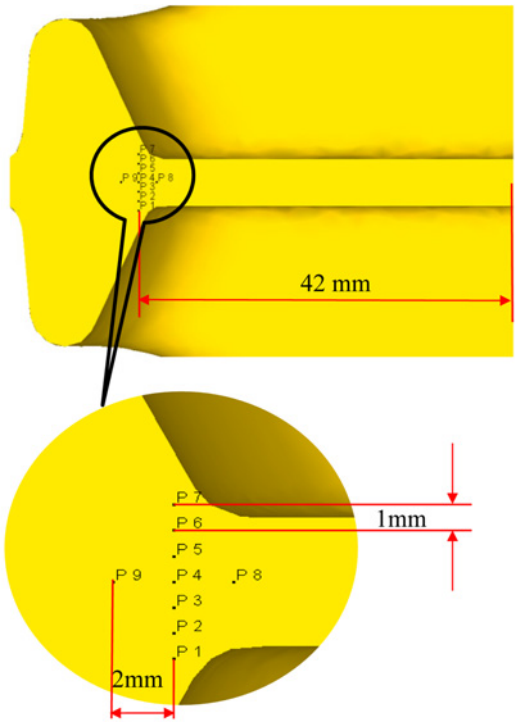

Fig. 14 Distribution of points whose flow velocities were measured

amplitude greater than 50%. The velocity decreased gradually from the middle to both sides along the vertical line. The velocity differences of P4-P5, P5-P6, and P6-P7 were calculated by considering only the symmetrical distribution, and the corresponding velocity differences are shown in Table 3. In general, the velocity differences in the design with UTF were smaller than those in the other two designs, and the value of P6-P7 is close to that of P5-P6, which explains the uniformity in velocity distribution in the design with UTF. In the region around P6 and P7, where cracks formed easily, the velocity difference in this dangerous area in the design with UTF decreased to 27.2% of the initial design, which reduces the risk of cracks significantly.

Based on the discussion above, the design with unequal thickness flash was chosen for optimal forging.

4. Process Stability Analysis

In practice, the forging stroke, friction condition, and workpiece mass are not always controlled precisely, especially in hot forging. Furthermore, the preform is not centered easily on the final forging die, especially when it is transferred manually. Therefore, the effect of different process parameters on the improved forging process with unequal thickness flash was analyzed by FE simulation.

Table 3 Velocity differences for different designs

Design schemes	Velocity differences (mm/s)		
	P4-P5	P5-P6	P6-P7
Design with damping grooves	7.6	24.1	61.0
Design with unequal flash thickness	3.1	19.4	22.0
Initial design	12.5	39.2	80.9

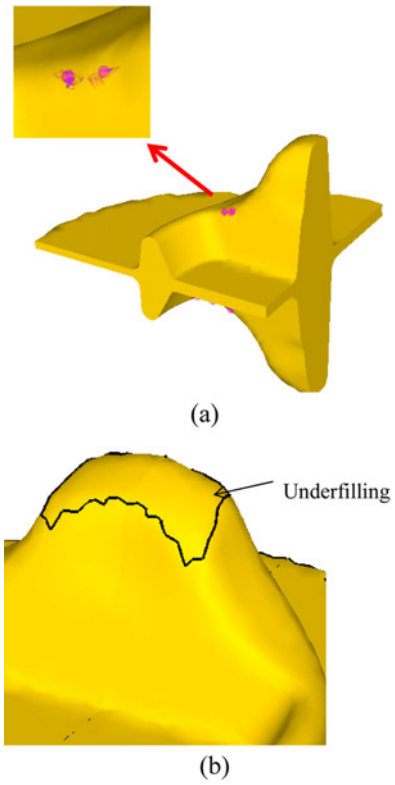

Fig. 15 Defects of scheme under different strokes: (a) folding defects, (b) underfilling

4.1 Influence of pre-upsetting stroke

The degree of bulking of the cylindrical preform is determined directly by the pre-upsetting stroke, which can influence the forming effect of final forging. To find an appropriate value of the pre-upsetting stroke *S*, strokes of 5.0, 20.0, and 35.0 mm were selected for simulation. When *S* was equal to 5.0 mm, folding defects were predicted in the transition area between the rib and fork parts, as presented in Fig. 15(a). It was easy to fill the metal with fork because of the relative higher preform. Some of the metal flowed back after the fork had formed, which resulted in folding. When *S* was equal to 20.0 mm, no folding defects resulted and the fork was well-filled. When *S* increased to 35.0 mm, an underfilling of the fork part occurred, as shown in Fig. 15(b). A large upsetting stroke increased the preform diameter. More material

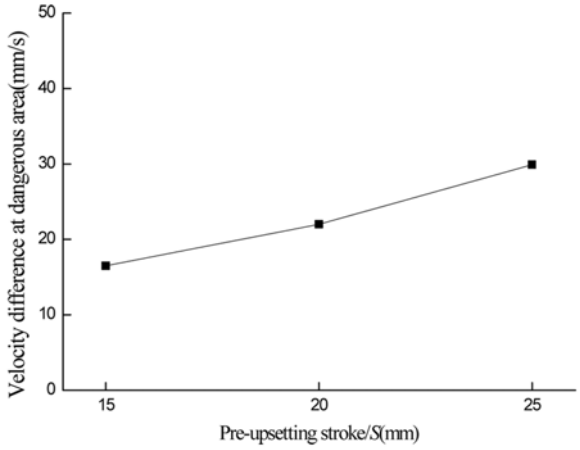

Fig. 16 The velocity difference at dangerous area under different pre-upsetting strokes

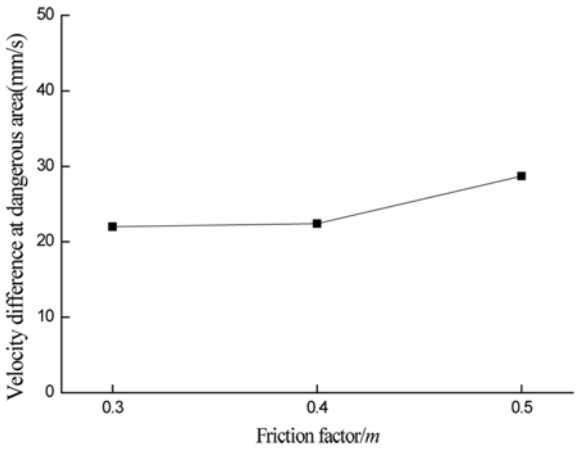

Fig. 17 The velocity difference at dangerous area with different friction factors

could therefore flow in the radial direction during final forging to form the flash and cause underfilling of the fork part.

A further two simulations with 15.0 and 25.0 mm pre-upsetting strokes were carried out. There was no folding and underfilling on the final forging. As shown in Fig. 16, the velocity difference in the dangerous area (P6-P7) increased with pre-upsetting stroke. The velocity difference reached 30.0 mm/s when S was equal to 20.0 mm, but the value is still less than half that of the initial design.

4.2 Influence of friction factor

During hot forging, lubrication conditions can be changed by many factors including lubricating coating, die surface, and oxide scale. In the FE model, lubrication conditions were established using a hypothetical friction factor. Therefore, it is necessary to discuss the simulation results using different friction factors. As reported in previous research[10], the friction factor (m) between the workpiece and dies increased from 0.3 to 0.5 as the oxide scale thickness decreased from 300 to 95 μm. Consequently, FE simulations were performed with friction factors of 0.4 and 0.5.

Folding and underfilling defects did not occur in the simulation. As shown in Fig. 17, the velocity difference at the dangerous area increased with friction factor. The friction resistance between the workpiece and die surface increases with friction factor, and results in a decrease in metal flow velocity near the die surface. In this case, the flow velocity at P7 would decrease, and the velocity difference between P6 and P7 increased.

4.3 Influence of workpiece mass

In mass production, the workpiece was sawed from a cylindrical bar, and the error in workpiece mass was controlled within 3%. Therefore, the tolerances of workpiece length, which can lead to a mass variation, should be controlled below 3%. Workpieces of different lengths, such as 97.0 mm (3%), 103.0 mm (+3%), and 95.0 mm (5%), were therefore used in the FE simulations.

For a fixed pre-upsetting, the bulging degree of preform increases with decrease in workpiece length (l). More material flows in the radial direction during final forging and the risk of underfilling increases.

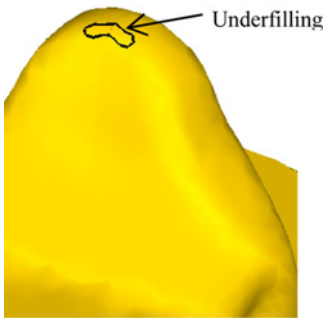

Fig. 18 The underfilling defects when the workpiece length was 95 mm

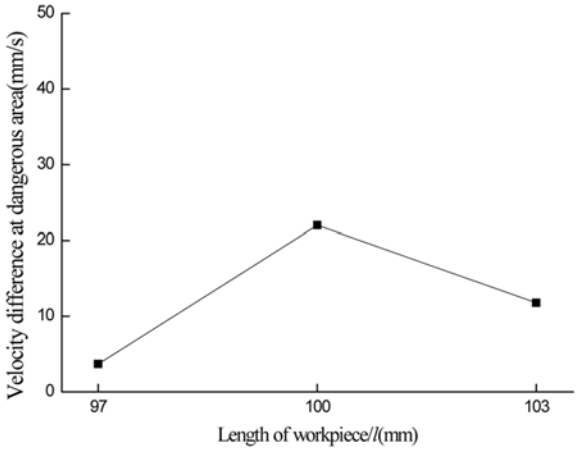

Fig. 19 The velocity difference at dangerous area of workpieces with different lengths

Underfilling occurs when the workpiece length is 95 mm, as shown in Fig. 18. The velocity difference in the dangerous area was also investigated, and the relationship between the velocity difference and workpiece length is presented in Fig. 19. When the error of mass was

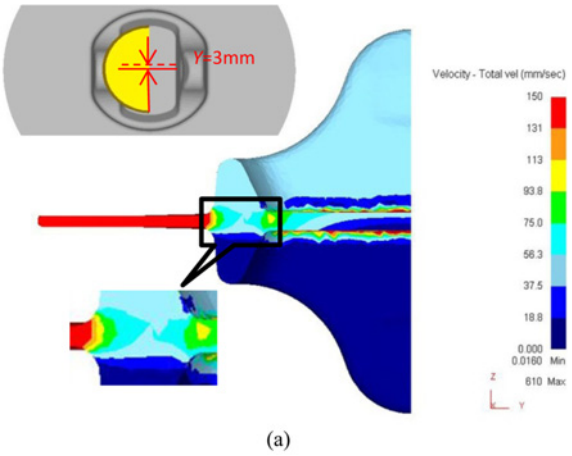

(a)

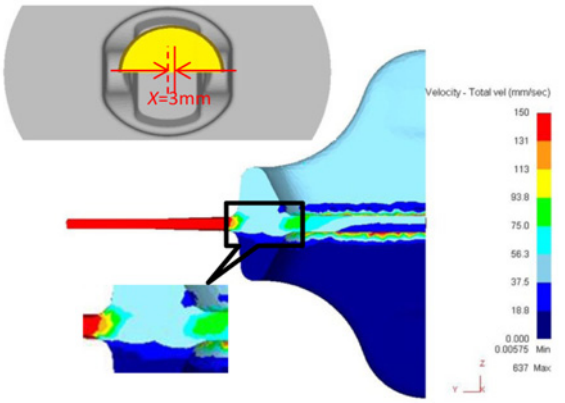

(b)

Fig. 20 Velocity distributions for different position of preform: (a) 3 mm offset along long-side, (b) 3 mm offset along short-side

3%, i.e., *l* was 97.0 mm, at the end of final forging, not much metal could flow to form the flash, so the entire flow trend decreased and this contributes to a decrease in velocity difference. When the error of mass was 3%, i.e., *l* was 103.0 mm, the fork part of the die was easier to fill, the already formed fork part could block metal flow at the dangerous area, and the velocity difference decreased.

4.4 Influence of preform position

During manual operation, it is not easy to place the preform in the correct position on the final forging die. This explains the asymmetric flash shape in the real forging in Fig. 6. Simulation results with different preform positions along the long and short sides of the inner die were therefore investigated, and the positioning offset from the center was set as 3 mm, as shown in Fig. 20. Folding and underfilling defects did not exist. The velocity distributions in Fig. 20 were similar to those in Fig. 12(b), which helps prevent surface crack formation during forging.

In summary, when the pre-upsetting stroke is 15.0~25.0 mm, the friction factor is 0.3~0.5, the error in mass is 3~3%, the positioning offset is 3 mm, and no folding and underfilling defects result in forging. For further analysis, data of the average velocity and the velocity difference at the dangerous area in the UTF design for different process parameters are plotted in Fig. 21, and the velocity values of the initial design are also provided as reference. Although the velocity values vary with fluctuations in the above four process parameters in the UTF

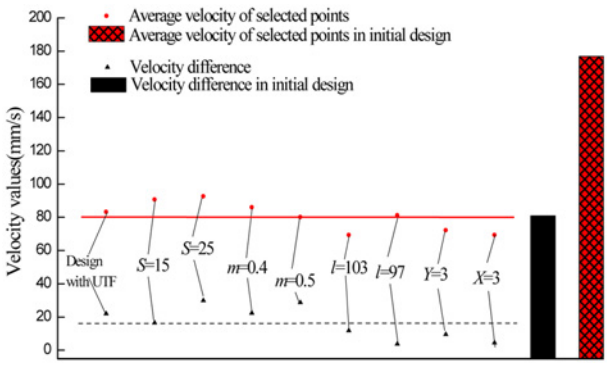

Fig. 21 Velocity values of different schemes

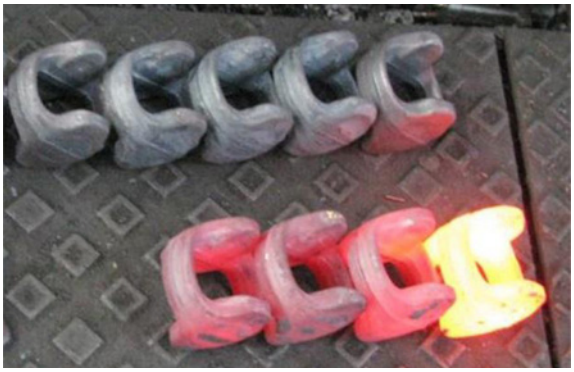

Fig. 22 Parts in the trial production

design, the absolute average velocity and velocity difference are much smaller than those of the initial design. The uniformity in velocity distribution has been improved and the risk of surface crack formation can be reduced. It can therefore be concluded that the proposed two-step forging process including pre-upsetting and final forging with UTF exhibits good process stability.

5. Trial Production

After evaluation of the process stability, the proposed design with UTF was applied in practical trial production. Workpieces with a target length of 100.0 mm were sawed from 70.0 mm round bars, and heated to 1200°C through an induction heating furnace. They were upset with a 20.0 mm stroke, and then deformed on the final forging die with an unequal flash gutter depth. After forging, the slug and flash were hot punched directly on another press, as shown in Fig. 22. After cooling to room temperature, all parts were sent for magnetic particle inspection, and it was found that crack defects did not occur in the initial process. Therefore, the feasibility and stability of the proposed process were demonstrated.

The metal flow lines on the key cross sections after forging were also investigated. The flow lines on cross-section S1 in Fig. 23(a) are reasonable, and crack traces, which appeared in the initial design shown in Fig. 23(b), are not visible. If we consider the adverse effect of punching on surface cracks, this result verifies the process feasibility.

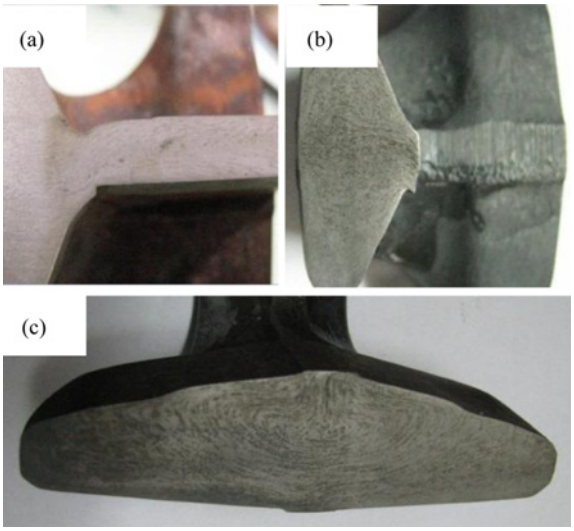

Fig. 23 Metal flow lines in initial and optimized processer: (a) cross-section S1 before punching in improved design, (b) cross-section S1 after punching in design with UTF, (c) cross-section S2 after punching in design with UTF

We can also prove the main reason for the cracking, which we tried to analyze previously, and we can also prove that the method to improve the flow velocity distribution and reduce the risk of crack formation by this forging method is effective.

The flow lines on cross-section S2 are shown in Fig. 23(c). Compared with the flow lines of the initial design in Fig. 7, the flow line distribution in the design with UTF is more reasonable. The accumulation of flow lines decreases, the directionality of their distribution is reduced significantly, and their degree of inward bending decreased. This could benefit the mechanical properties of the duplex fork.

6. Conclusions

The crack defects on the duplex fork in the initial process were observed and the main reason for surface crack formation was discussed in detail based on the FE simulation. The non-uniform velocity distribution in the transition between the slug and rib and the large velocity difference generated additional tensile stresses. A large amount of oxide scale was generated during the one-step forging process, and a large amount of material flow caused oxide scale flow. The brittle oxide scale was broken easily, and some of the harder oxide scale pierced the soft metal surface to form high level tensile stress, which resulted in surface crack formation.

An optimized two-step forging process was developed. Most oxide scale generated from heating was removed by pre-upsetting, and its adverse effect on final forging could be prevented. Final forging with unequal thickness in flash design improved the uniformity of velocity distribution on the key cross section and decreased the velocity difference in the dangerous area. As a result, the risk of surface crack formation on the forging part was reduced and crack-free forgings of the duplex fork were obtained in successive trial production.

By considering flexible conditions in real forging, the effect of different process parameters (including the pre-upsetting stroke, friction factor, mass of workpiece, and preform positioning offset) on the optimized forging process were analyzed by FEM. Process stability of the proposed design was achieved with unequal thickness flash.

The velocity distribution was effective as an evaluation index to avoid crack defects of the duplex fork and optimize the forging process. Compared with the damage analysis method, this method is less time consuming and relatively easy to carry out. This method can probably be applied to other similar forging parts.

ACKNOWLEDGEMENT

This work was partially supported by the National Natural Science Foundation of China (No. 51475294).

REFERENCES

1. Bulut, G. and Parlar, Z., “Dynamic Stability of a Shaft System Connected through a Hooke's Joint,” Mechanism and Machine Theory, Vol. 46, No. 11, pp. 1689-1695, 2011.
2. Khalilpourazary, S., Dadvand, A., Azdast, T., and Sadeghi, M. H., “Design and Manufacturing of a Straight Bevel Gear in Hot Precision Forging Process using Finite Volume Method and CAD/CAE Technology,” The International Journal of Advanced Manufacturing Technology, Vol. 56, No. 1-4, pp. 87-95, 2011.
3. Zhang, Y., Shan, D., and Xu, F., “Flow Lines Control of Disk Structure with Complex Shape in Isothermal Precision Forging,” Journal of Materials Processing Technology, Vol. 209, No. 2, pp. 745-753, 2009.
4. Kim, J.-B., Seo, W.-S., and Park, K., “Damage Prediction in the Multistep Forging Process of Subminiature Screws,” Int. J. Precis. Eng. Manuf., Vol. 13, No. 9, pp. 1619-1624, 2012.
5. Duan, X. and Liu, J., “Research on Damage Evolution and Damage Model of 316LN Steel during Forging,” Materials Science and Engineering: A, Vol. 588, pp. 265-271, 2013.
6. Rao, A. V. and Ramakrishnan, N., “A Comparative Evaluation of the Theoretical Failure Criteria for Workability in Cold Forging,” Journal of Materials Processing Technology, Vol. 142, No. 1, pp. 29-42, 2003.
7. Arentoft, M., Henningsen, P., Bay, N., and Wanheim, T., “Simulation of Defects in Metal Forming-An Example,” Journal of Materials Processing Technology, Vol. 45, No. 1, pp. 527-532, 1994.
8. Joun, M. S., Lee, S. W., and Chung, J. H., “Finite Element Analysis of a Multi-Stage Axisymmetric Forging Process Having a Spring-Attached Die for Controlling Metal Flow Lines,” International Journal of Machine Tools and Manufacture, Vol. 38, No. 7, pp. 843-854, 1998.
9. Abdullah, A. B., Sapuan, S. M., Samad, Z., Khaleed, H. M. T., and Aziz, N. A., “Numerical Investigation of Geometrical Defect in Cold

Forging of an AUV Blade Pin Head," Journal of Manufacturing Processes, Vol. 15, No. 1, pp. 141-150, 2013.

10. Matsumoto, R., Osumi, Y., and Utsunomiya, H., "Reduction of Friction of Steel Covered with Oxide Scale in Hot Forging," Journal of Materials Processing Technology, Vol. 214, No. 3, pp. 651-659, 2014.
11. Daouben, E., Dubois, A., Dubar, M., Dubar, L., Deltombe, R., et al., "Effects of Lubricant and Lubrication Parameters on Friction during Hot Steel Forging," International Journal of Material Forming, Vol. 1, No. 1, pp. 1223-1226, 2008.
12. Torres, M. n. and Colás, R., "A Model for Heat Conduction through the Oxide Layer of Steel during Hot Rolling," Journal of Materials Processing Technology, Vol. 105, No. 3, pp. 258-263, 2000.
13. Suarez, L., Rodriguez-Calvillo, P., Houbaert, Y., Garza-Montes-de-Oca, N. F., and Colas, R., "Analysis of Deformed Oxide Layers Grown on Steel," Oxidation of Metals, Vol. 75, No. 5-6, pp. 281-295, 2011.
14. Scarabello, D., Ghiotti, A., and Bruschi, S., "FE Modelling of Large Ingot Hot Forging," International Journal of Material Forming, Vol. 3, No. 1, pp. 335-338, 2010.
15. Li, Y. H. and Sellars, C. M., "Comparative Investigations of Interfacial Heat Transfer Behaviour during Hot Forging and Rolling of Steel with Oxide Scale Formation," Journal of Materials Processing Technology, Vol. 80, No. pp. 282-286, 1998.
16. Kchaou, M., Elleuch, R., Desplanques, Y., Boidin, X., and Degallaix, G., "Failure Mechanisms of H13 Die on Relation to the Forging Process-A Case Study of Brass Gas Valves," Engineering Failure Analysis, Vol. 17, No. 2, pp. 403-415, 2010.
17. Chavoshi, S. Z., Tajdari, M., and Luo, X., "An Investigation into the Effect of Variable Flash Thickness on the Strength of an AA7075 Part Obtained by Hot Closed-Die Forging," Proceedings of the Institution of Mechanical Engineers, Part C: Journal of Mechanical Engineering Science, DOI No. 10.1177/0954406214540284, 2014.
18. Grass, H., Krempaszky, C., and Werner, E., "3-D FEM-Simulation of Hot Forming Processes for the Production of a Connecting Rod," Computational Materials Science, Vol. 36, No. 4, pp. 480-489, 2006.
19. Zhang, Y.-J., Hui, W.-J., and Dong, H., "Hot Forging Simulation Analysis and Application of Microalloyed Steel Crankshaft," Journal of Iron and Steel Research, International, Vol. 14, No. 5, pp. 189-194, 2007.
20. Tomov, B., Radev, R., and Gagov, V., "Influence of Flash Design upon Process Parameters of Hot Die Forging," Journal of Materials Processing Technology, Vols. 157-158, pp. 620-623, 2004.